STUDY OF A PHENOMENOLOGICAL MODEL FOR ELASTOMERIC BEARINGS

C. Casarotti[1] and A. Pavese[2]

[1] *Researcher, European Centre for Training and Research in Earthquake Engineering, Pavia. Italy*
[2] *Professor, Dept. of Structural Mechanics, University of Pavia, Pavia, Italy*
Email: chiara.casarotti@eucentre.it, a.pavese@unipv.it

ABSTRACT :

Elastomeric bearings are one of the most commonly used seismic isolators, whose considerably grown number of applications in recent years witnesses the confidence in seismic isolation. On the other hand, full-scale experimentation of isolators, so far conducted in a limited number of international facilities, focused the attention to unexpected collapses, highlighting how the assessment of the seismic behavior of base-isolated structures strongly depends on the accuracy of the isolators modeling. With some exception, models present in literature are generally intended to represent the overall isolator behavior, without information on the state of internal layers, where some rubber layer may show high deformations that can unevenly damage the layer itself and influence the global stress distribution. The main objective of the present work is to develop a phenomenological model able to represent the force-deformation state of each layer of the device. The proposed model includes geometric nonlinearities in the formulation and material nonlinearities in the constitutive laws, defined by a number of parameters which are calibrated coupling a system identification approach and a sensitivity analysis in the interpretation of the experimental test results on full-scale bearings carried out at the EUCENTRE TREES Lab of Pavia (Italy). The model is found suitable to represent the experimental response.

KEYWORDS: Rubber bearings, analytical model, seismic isolation, experiments, shake table

1. INTRODUCTION

Nowadays, the use of base isolation within the Italian and European context is gaining more and more acknowledgement, thanks to the high level of protection which can be guaranteed to a structure from the earthquake damage. The fact that the production of such devices is fully dependent on industrial manufacturing processes, with the consequent possibility of standardization and quality control, renders seismic isolation a technological solution particularly appealing from the point of view of the structural safety. Elastomeric bearings are one of the most commonly used seismic isolators, and the considerably grown number of applications in recent years witnesses the confidence of the modern engineer with such design approach. On the other hand, full-scale experimentation of isolation devices, so far conducted in a limited number of international experimental facilities, has focused the attention to unexpected collapses, basically due to the influence on the device response of a number of factors usually neglected in the current state of practice, to scale effects of full scale devices, to assemblage effects of complex devices and to the unavoidable percentage of random variations in mechanical characteristics ascribable to the operating conditions or manufacturing dispersions.
The response of elastomeric isolators is inherently nonlinear as a result of a number of factors like scragging, temperature, axial load, geometric effects, among the others (e.g. Benzoni and Casarotti, 2005, Yakut and Yura, 2002, Yoo *et al.*, 2000). Besides factors inherent to the physical nature of the device, variables exist related to manufacturing processes and materials, random in nature, such as the types of employed adhesives, the molding homogeneity, the vulcanization procedures and conditions, which may affect the effectiveness of the steel-elastomer bonding, eventually modifying the bearing response or cause premature collapses.
All of the above considerations highlight how the assessment of the seismic behavior of base-isolated structures strongly depends on the accuracy of the modeling of the isolators. The most of models present in literature can be roughly subdivided in finite element models and in analytical phenomenological models. In the former category, several thousands of solid finite elements are used for the modeling of rubber, steel plates, shims and

lead core, while constitutive laws at different level of complexity are studied (e.g. Takhirov and Kelly, 2006, Doudoumis *et al.*, 2005, Ali *et al.*, 1995). The large part of models belonging to the latter category are represented by analytical laws of different kind, i.e. hysteretic models (Hwang *et al.*, 2002, Hwang and Hsu, 2001, Kikhuci and Aiken, 1997), buckling models (Ryan et al., 2005, Nagarajaiah and Ferrell, 1999, Koh and Kelly, 1988) or other kind of macro models (Iizuka, 2000).
With the exception of Chang (2002), all of the latter models aim to represent the overall isolator behavior, without information on the state of internal layers. However, some rubber layer often appears to have high deformations and can be unevenly damaged, modifying the global stress distribution. This phenomenon is due to both the tilting of the middle bearing layers when the bearing is deformed in shear and to the small variations of mechanical characteristics and geometric imperfection of the steel and rubber layers. Such variations, which may localize high deformations, are ascribable to the operating conditions or more simply to the manufacturing dispersions, and thus they appear random in nature. In order to obtain a reliable prediction of the device response, the model of the bearing has (i) to be able to represent the global response and (ii) to allow simulating the uneven random distribution of mechanical characteristics within the isolator itself.
The main objective of the present work is to develop a phenomenological model able to reproduce the force-deformation state of each layer of the device, which may constitute the base for a probabilistic modeling of the isolator, aimed at estimating the probability occurrence of possible collapses. The proposed model includes geometric nonlinearities in the formulation and material nonlinearities in the constitutive law of the layers, defined by a number of parameters which are calibrated coupling a system identification approach and a global sensitivity analysis in the interpretation of the experimental test results on full-scale bearings carried out at the EUCENTRE TREES Lab of Pavia (Italy). Once the methodology is defined and verified, it can be extended to further developments of the constitutive laws of the materials.

2. ANALITYCAL MODEL DEVELOPMENT

The object of the present work is to develop a relatively simple but complete model of a multilayer rubber bearing isolator, able to reproduce both the overall response and the single layer loading state. The phenomenological model has been developed with the following concepts in mind: (i) the multilayer formulation, (ii) the consideration of three degrees of freedom (dofs) per layer, (iii) the inclusion of large displacements, (iv) the inclusion of nonlinear stiffnesses. The idea is to model each single layer and to join them in series. The nonlinear analytical model developed for the single layer is based on the Koh and Kelly (1988) linear model and on the further developments by Nagarajaiah and Ferrell (1999), consisting in coupling a shear and a rotational spring, with non-linear stiffnesses and considering large displacements.
In the proposed model, each layer has the shear dof, s, represented by a nonlinear shear spring of stiffness K_h, the axial dof, t, represented by a nonlinear spring of stiffness K_v, and the rotational dof, θ, i.e. the overall rotation of the layer. Layers are interconnected by means of rotational springs of tilting stiffness K_θ, (figure 1).

2.1. Device Equilibrium Equations and Model implementation

The equilibrium equations for each layer of the isolator are obtained by means of the theorem of virtual displacements applied to the whole system: for equilibrium to be ensured the total potential energy Π must be stationary for variations of admissible displacements. The total potential energy of a n layers isolator can be expressed as the sum of the contributions of each single layer i:

$$\Pi = \frac{1}{2}\sum_{i=1}^{n+1} K_{\theta i}(\theta_i - \theta_{i-1})^2 + \frac{1}{2}\sum_{i=1}^{n} K_{hi}(s_i)^2 + \frac{1}{2}\sum_{i=1}^{n} K_{vi}(t_i)^2 - Ph - Fu \qquad (2.1)$$

where u and h are the horizontal and vertical top displacements (i.e. in global coordinates), respectively. Such displacements are given by the sum of single layers displacements u_i and h_i in the global reference system, which are univocal function of the layer displacements and height l_i, as shown in figure 1:

$$u=\sum_{i=1}^{n}u_i=\sum_{i=1}^{n}\left((l_i-t_i)\sin\theta_i+s_i\cos\theta_i\right)$$
$$h=\sum_{i=1}^{n}h_i=\sum_{i=1}^{n}\left(l_i-l_i\cos\theta_i+s_i\sin\theta_i+t_i\cos\theta_i\right) \tag{2.2}$$

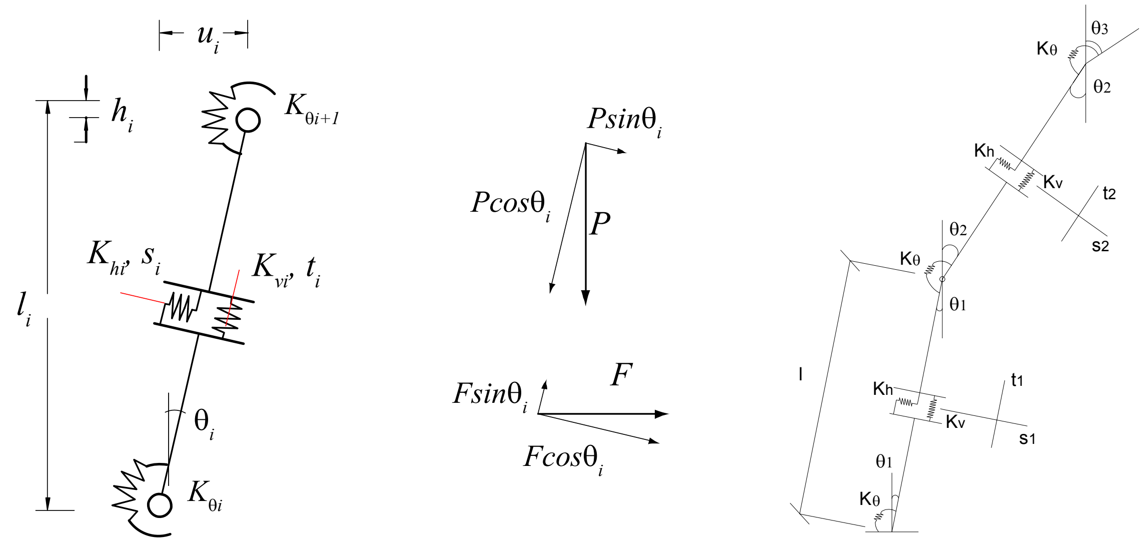

Figure 1 isolator model: single layer (left) and layers in series (right)

The model has $n+1$ rotational springs, since the rotation of each layers is considered uniform, and the effects of such rotations are concentrated at the extremities of each layer in the connection rotational springs. Boundary conditions are no translations of the base extremity and no rotations at the base and at the top of the isolator (i.e. $\theta_0 = \theta_{n+1} = 0$), reasonable condition for bearings with steel top and bottom plates. The shear, axial and rotational equilibrium of each layer is obtained by imposing the stationarity of Π with respect to the ith displacements s_i, t_i and θ_i (Zienkiewicz and Taylor, 2000). The system is in general subjected to a given vertical load P (constant or variable), and the horizontal displacement u imposed at the top. This imply that the system has totally $3n+1$ unknowns, i.e. the three relative displacements of each layer and the output force F at the top, for a total of the $3n+1$ equations:

$$f_{3i-2}=\frac{\partial\Pi}{\partial s_i}=K_{hi}s_i-P\frac{\partial h}{\partial s_i}-F\frac{\partial u}{\partial s_i}=K_{hi}s_i-F\cos\theta_i-Psen\theta_i=0$$
$$f_{3i-1}=\frac{\partial\Pi}{\partial t_i}=K_{vi}t_i-P\frac{\partial h}{\partial t_i}-F\frac{\partial u}{\partial t_i}=K_{vi}t_i+Fsen\theta_i-P\cos\theta_i=0$$
$$f_{3i}=\frac{\partial\Pi}{\partial\theta_i}=K_{\theta i}(\theta_i-\theta_{i-1})-K_{\theta i+1}(\theta_{i+1}-\theta_i)-P\frac{\partial h}{\partial\theta_i}-F\frac{\partial u}{\partial\theta_i}=\dots \tag{2.3}$$
$$\dots=K_{\theta i}(\theta_i-\theta_{i-1})-K_{\theta i+1}(\theta_{i+1}-\theta_i)-P((l_i-t_i)\sin\theta_i+s_i\cos\theta_i)-F((l_i-t_i)\cos\theta_i-s_i\sin\theta_i)=0$$
$$f_{3n+1}=u-\sum_{i=1}^{n}\left((l_i-t_i)\sin\theta_i+s_i\cos\theta_i\right)=0$$

The model has been implemented using MATLAB software (The MathWorks, 2007). The system equilibrium equations are written in the deformed configuration at each step, without any linearization and/or small displacement assumption, fully accounting for geometric nonlinearity. The nonlinearity of the system response requires an iterative step by step solution of the equilibrium equations, for which the MATLAB function *fsolve* has been employed. The model has the following unknown vector:

$$x = \{s_1, t_1, \theta_1, \cdots, s_n, t_n, \theta_n, F\}^t \quad (2.4)$$

For sake of computational saving, the Jacobian of the system of equations has been analytically computed, in order to make the algorithm converge faster.

2.3 Linear and nonlinear material properties

Often, the actual elastomer properties are not available, and even when they are available the bearings usually have different properties than the small elastomer specimen used to determine basic properties, as observed by Koh and Kelly (1988) in past experiments. In the present work, initial isolator elastic stiffnesses are estimated from nominal values of the rubber properties, considering a margin of variability, and are associated with nonlinear stiffness variations defined by nonlinear relationships.
At a first step, each layer is characterized by a set of initial (elastic) stiffness properties. In the case of horizontal and vertical stiffness, K_{0h} and K_{0v}, general agreement is found (e.g. Skinner *et al.*, 1993):

$$K_{0hi} = \frac{GA}{l_{ri}} \quad ; \quad K_{0vi} = \frac{6GS_i^2 Ak}{(6GS_i^2 + k)l_{ri}} \quad (2.5)$$

where G and k are the rubber shear and bulk moduli, l_{ri}, S_i and A are the rubber layer thickness, shape factor and area. It has to be noted that the rubber bearing rotational stiffness is not a common design parameter and in literature some relation can be found for the whole isolator (e.g. Nagarajaiah and Ferrell, 1999, Iizuka, 2000, Jaishi and Ren, 2007) or for single layers (Chang, 2002), but there is no general agreement. For the present model, the rotational stiffness is concentrated between layers, that means that the layer rotational stiffness has to be sort of 'translated' to an interface tilting stiffness, considering the different conditions at the top and bottom plate of the isolator. From very basic considerations, the tilting stiffness at the top and bottom plates interface is taken twice the stiffness between inner layers. Since the scope is to optimize parameters characterizing the stiffness, the simplest and most intuitive relationship, among the ones found in literature, has been chosen for the initial value $K_{\theta 0}$ (Jaishi and Ren, 2007):

$$K_{0\theta i} = \frac{K_{0vi} B^2}{2} \quad (2.6)$$

where B is the bearing plan dimension. Based on the observation of the experimental response, nonlinear stiffnesess have been modeled. In particular it is observed a softening in the shear stiffness with shear strain, while the vertical stiffness increases with compressive displacement. For the current value of the vertical stiffness K_v, the authors suggest a relationship similar to the one employed by Nagarajaiah and Ferrell (1999) for horizontal stiffness, also considering that the stiffness increase should be limited:

$$\frac{K_v}{K_{v0}} = (1 + p_2 \tanh(p_3 \frac{t}{l_r})) \quad (2.6)$$

where, p_2 represents the final stiffness increment (e.g. $p_2 = 0.6$ means a stiffness increment of 60%), while p_3 represents the rate of stiffness increment with the axial deformation.
For non-cyclic test, i.e. without modeling hysteretic behavior, a law for the variation of nonlinear shear stiffness, K_h, as a function of shear deformation, is found in Nagarajaiah and Ferrell (1999):

$$\frac{K_h}{K_{h0}} = (1 - p_5 \tanh(p_6 \frac{s}{l_r})) \quad (2.7)$$

where p_5 represents the final stiffness decay, while p_6 represents the rate of stiffness decay with the shear deformation. Figure 2 shows results of compression and shear tests on two isolators of the same type. Solid lines represent the actual stiffness, while dashed lines represent a 'manual' fitting (i.e. with parameters roughly set manually) given by the analytical relationship: it can be noted that the given law represents fairly well the stiffness encountered in experimental data.

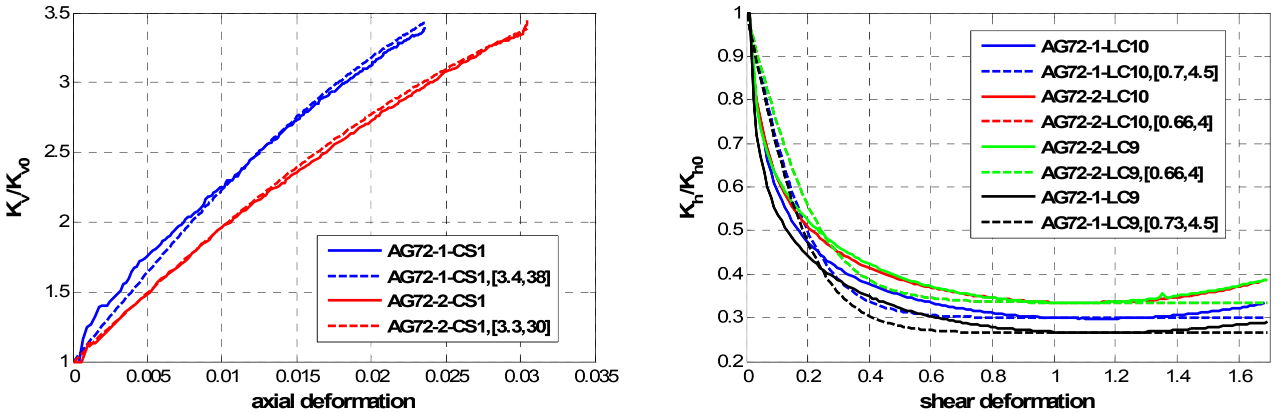

Figure 2 Vertical (left) and horizontal (right) stiffness variation with strain: experimental versus analytical

Direct measure of rotational stiffness is not available. According to the relationship suggested by Nagarajaiah and Ferrell (1999), the following function has been employed:

$$\frac{K_\theta}{K_{\theta 0}} = (1 - p_8 \frac{s}{l_r}) \quad (2.5)$$

where $1/p_8$ represents the value of shear strain corresponding to zero rotational stiffness, which may represent the device instability (rollover). Since such decay is not limited, in order to avoid negative stiffness, caution has to be made in selecting $1/p_8$ always greater than the maximum expected shear strain. Investigation is needed in order to experimentally characterize such stiffness.

3. MODEL CALIBRATION METHODOLOGY

The implemented procedure consists of coupling a system identification approach and a sensitivity analysis in the interpretation of the experimental test results: the fitting between experimental response and numerical prediction is used to optimize parameters, and the variations in the simulated response are used for the sensitivity study. Since general closed form solutions are not available relating directly the material parameters to the bearing response, parametric analyses using the numerical model have been performed and well-known optimization techniques (e.g. Tarantola, 2004) have been applied.
Experimental tests were conducted at the TREES Lab of EUCENTRE (Pavia, Italy), on the Bearing Tester System, one of the few large bearing testing machines in the world. The customized design of the actuation system and the control software allows performing biaxial test on real scale bearings in static and dynamic conditions. All the measurable quantities of the specimens are estimated, i.e. geometric data and some material property. Tests can be basically described as application of a 1D input and the observation of a 1D output: the input and output of the vertical test are the imposed compressive force centered at the bearing

top, and the resulting vertical displacement, respectively, while for the horizontal test they are the imposed displacement at the bearing top, and the corresponding measured restoring force. The recorded experimental input is then applied to the numerical model to get a synthetic output.
The direct construction of the probabilistic model of all the parameters of the analytical model is impossible due to the lack of data and the high number of uncertain parameters. A probabilistic model of the stiffness characteristics is thus defined by a number of parameters. Both the sensitivity analysis and the data inversion are based on a multiple solution of the forward problem, i.e. estimating the response from the input and the model parameters. In order to check the quality of the model and of the knowledge of the parameters, initial deterministic simulations are run with parameters estimated by engineering measures and judgment.
A scheme of the applied methodology is depicted in figure 3. A probability distribution is defined for each of the model parameters: rather large uniform distributions are selected, within credible upper and lower bounds, to describe the a priori information about the different parameters. A Monte Carlo (MC) sample is generated, sampling the distribution of the different parameters. Each set of model parameters is then associated to the corresponding simulated output, which constitute the base for the sensitivity analysis.
Two schemes have been followed, consisting of two distinct phases: a coarse (or global) optimization scheme (Phase I) and a fine (or local) search scheme (Phase II). For each model, a scalar misfit function is determined based on the series of the difference between observed and simulated output. The misfit distribution is analyzed to identify models with the lowest misfit, whose parameters are considered optimal. A scatter-plot is produced for each parameter, plotting the value of the individual parameter versus the corresponding misfit, in order to visually analyze the impact of such parameter on the goodness of the prediction, despite the values assumed by the others. Phase I aims at determining promising subregions of the complete search space within which optimal models might be located. In this phase, parameters effectively influencing the response are identified. Some parameters will likely have a significantly higher influence than others, thus completely hiding the importance of the latter. A sensitivity analysis is then carried out in order to detect secondary but still important parameters for new calibration: Phase II aims at refining the results of phase I and at selecting the optimum model in a suitably defined neighborhood of each initial solution (as provided by phase I).
Once optimal numerical parameters are identified for a large number of isolators, the subsequent step will be to correlate them to the physical and mechanical (i.e. measurable) properties of the bearings.

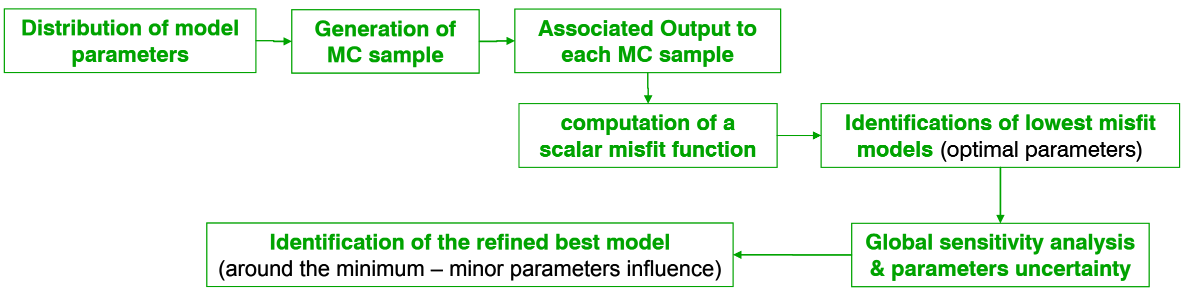

Figure 3 Applied Methodology

3.1 Variation ranges of parameters

Initial values and variation laws for model stiffnesses are characterized by a vector of parameters $\underline{p}$, summarized in table 1, which will be optimized on bearings experimental response. In particular, also initial values of stiffnesses are taken as variable according to "initial stiffness multipliers" p_1, p_4 and p_7 for vertical, horizontal and rotational stiffnesses, respectively.
All parameters have been varied, in order to assess the impact of the uncertainty and to identify optimal values for the different parameters. To maintain the maximum generality and to minimize the imposed a priori information, parameter distributions are assumed uniform and in general independent, incorporating only strong physical constraints. Concerning initial estimates of the rubber stiffnesses, wide variation

ranges are considered because known relationships (axial and shear stiffness) are representative not of the very beginning value of the stiffness, but of the average stiffness in the medium deformation range. This means that the expected optimal values of the initial vertical and horizontal stiffnesses multipliers will be lower and higher than one, respectively, due to the presence of hardening and softening response, respectively. For the shear stiffness it has also to be observed that static tests are performed on unscragged devices, which may further justify the higher value of the initial stiffness. On the other hand, no experimental evidence on the rotational stiffness trend is known to the authors, for which reason the maximum generality is preferred, and the a priori "stiffness decay information" is preferred to be neglected, by considering also negative values of p_8. Variation ranges for nonlinear parameters, defined into table 3.1, are inferred from considerations on the numerical laws (Figure 4).

Table 3.1 Parameters Variation Ranges

Stiffness	K_v			K_h			K_θ	
Parameter	p_1	p_2	p_3	p_4	p_5	p_6	p_7	p_8
Range	0.02 – 1.2	0.05 – 15	2 - 80	0.5 – 3.5	0.1 – 0.9	0.3 - 5	0.05 – 2	-0.4 – 0.4

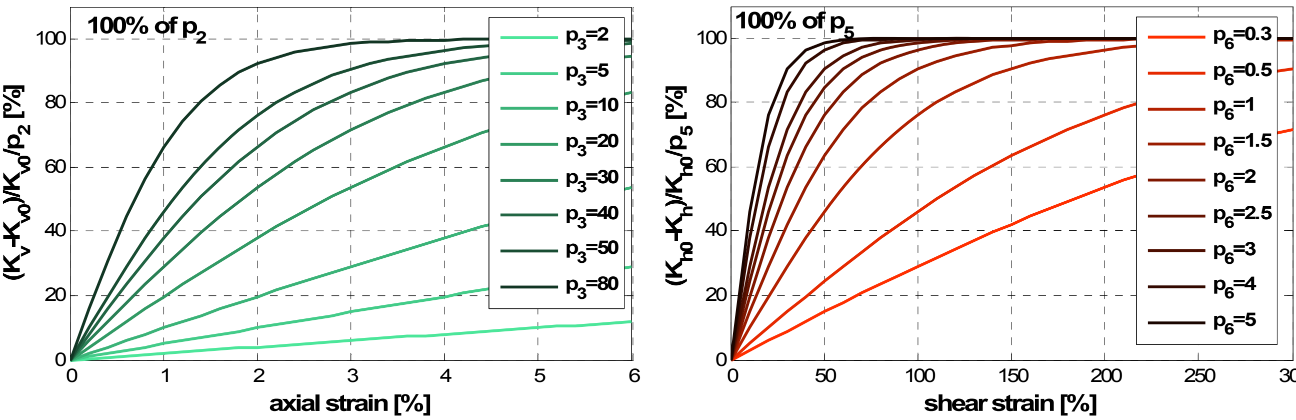

Figure 4 Percentage variation of axial (left) and shear (right) stiffnesses with deformation

Figure 4 (left) shows the axial stiffness percentage increasing with axial deformation up to 6%, and figure 4 (right) shows the shear stiffness percentage decay with shear deformation up to 300%: considering that the maximum stiffness decay is represented by parameter p_5, different values of parameter p_6 indicate the rate of such decay, i.e. higher values of p_6 means that K_h reaches a stable value of (1- p_5)K_{h0} for relatively low deformations, and viceversa lower values of p_6 imply a softer stiffness decay.

3.2 Global Search, Sensitivity analysis and Model Refinement

The response function is minimized by identifying an error function as the Root Mean Square (RMS) error of the response quantity R of interest throughout the N steps of the entire response (Eqn. 3.1). The presence of important minimum regions in the RMS error allows detecting important input parameters.

$$\varepsilon_{global} = \sqrt{\sum_{i=1}^{N} \left(R_{\exp,i} - R_{num,i}\right)^2 / N} \tag{3.1}$$

The RMS error, as defined throughout the entire response, with R varying from zero to the maximum value, gives higher importance to errors at large displacement/force amplitudes, which is desirable, since the matching of the response at larger displacements is of major interest.
On the basis of the results of phase I, which allows locating optimal values for primary parameters, sensitivity analysis is conducted at different levels of complexity, in order to rank parameters and detect

negligible parameters. Sensitivity Analysis determines the contribution of individual input variable to the uncertainty in model predictions. Prioritizing (ranking) factors means identifying factors which, if determined, would lead to the greatest reduction in the variance of the target output (Saltelli *et al.*, 2004). A proper ‘‘output screening’’ allows simplifying the model, by identifying factors fixable at any given value over their variation range without reducing significantly the output variance, i.e. without significant loss of information. When a Monte Carlo study is being performed, propagation of the sample through the model creates a mapping from analysis inputs to analysis results, which can be explored in many ways to determine the sensitivity of model predictions to individual input variables. The are a number of methods for Sensitivity analysis, some of which based on regression analysis and correlation measures (PEAR, PCC and SRC methods for linear models and their rank transformation SPEA, PRCC and SRRC for nonlinear models), other based on the analysis of the output variance, which basically allow not only estimating the main contribution of each individual parameter, but also detecting possible higher level interactions among parameters. Detailed discussion on the subject is found in Saltelli *et al.* (2004).
Scatter plots are used for visual assessment of the influence of individual inputs on an output and are often used as a first step in other more refined sensitivity analyses methods. In the scatter plots each point corresponds to a model (i.e. a set of model parameters), but it is representative of the influence of the single parameter: a minimum in the lower border of the RMS error scatter plot indicates that the parameter value corresponding to the misfit minimum allows achieving the best fit of the response. Whether the sensitivities of two inputs differ significantly from each other, they cannot always be judged from the visual inspection of scatter plots. This is the basic reason of the need of a subsequent more refined sensitivity analysis and/or local search around the minimum region. The response function is then calculated running numerical simulations in a limited neighborhood (the “minimum region” or “trust region”) of the main parameters influencing the model and a refined model is found corresponding to a minimum RMS error region also for secondary parameters.

4. MODEL CALIBRATION RESULTS BASED ON MONTE CARLO NUMERICAL SIMULATIONS

Optimization has been run on two statistically identical isolators (labelled RBA72), subjected to the following testing protocol: vertical stiffness test (test #1) with bearing loaded up to 2900 kN, and shear tests (test #2 and 3) with bearing laterally loaded up to 156 mm, at constant vertical load of 1800 and 2900 kN, respectively. The vertical test is used first to independently calibrate the vertical stiffness parameters, since there is no evident influence of horizontal and rotational stiffnesses on such tests. Once the set of vertical stiffness parameters are estimated, horizontal test results are used to calibrate other parameters.

4.1 Vertical test calibration

Vertical test are used to determine parameters p_1, p_2, p_3. Total model runs were 5000 per isolator. Figure 5 (left) shows the lowest error models (blue lines) compared with the experimental result (black line) and the worst prediction (green line) for one of the isolators. Statistics of numerical values of parameters and RMS error of the vertical displacement response for the best 20 models are listed in table 4.1. The vertical behavior is captured quite fairly, with RMS errors of 0.001-0.003 mm, calculated on the vertical displacement history with a maximum of 2-2.7 mm. Values are slightly different from one isolator to the other, for which reason average parameters values are used for the horizontal analysis, considering that vertical stiffness properties do not seem to have significant role in the horizontal response.
From scatterplot results (figure 5, right), it is found that the most influencing parameter is the initial stiffness multiplier p_1, for which a clear minimum region is detectable. However, for p_2 and p_3 a pattern is recognizable (in the upper bound region) even if a defined minimum cannot be identified. In order to localize the trust region for p_2 and p_3, it is desirable to restrict the p_1 variation range while varying the other two. Sensitivity analyses other than scatterplots are conducted using the software SimLab v2.2.1 (Saltelli et al., 2004). Sensitivity indexes estimated according to different methods (SPEA, PRCC and SRCC), give

results very similar, basically confirming the importance of the first parameter with respect to the others.

Table 4.1 Vertical test results: statistics of best 20 models

		p_1	p_2	p_3	*RMS* error [mm]
RBA72-1	Mean	0.20	5.76	30.73	0.0021
	Standard deviation	0.075	3.578	21.881	0.0007
	cov	37.13%	62.15%	71.22%	32.93%
RBA72-2	Mean	0.10	7.40	32.87	0.0031
	Standard deviation	0.050	4.130	16.486	0.0009
	cov	49.18%	55.81%	50.16%	29.51%

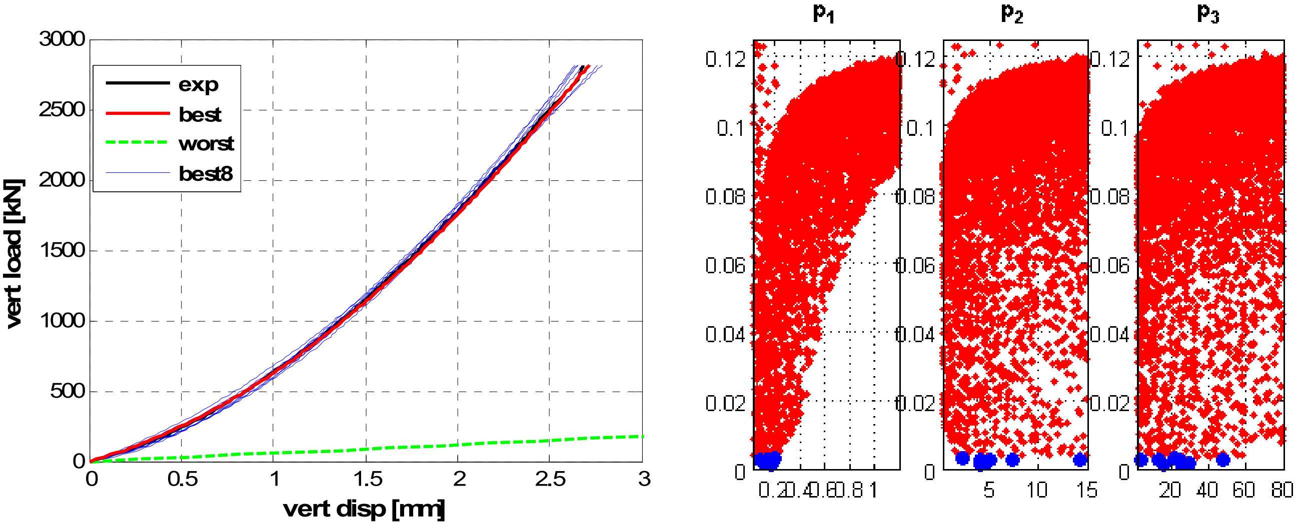

Figure 5 RBA72-2, test #1 (axial): best 8 models (left) and RMS scatterplots (right)

4.2 Horizontal test calibration

Horizontal analyses are run with given vertical stiffness parameters, in order to determine parameters p_4 to p_8. Total model runs were 6000 per test (two shear tests per isolator). Figure 6 (left) shows the lowest error models (blue lines) compared with the experimental result (black line) and the worst prediction (green line) for one of the isolators. Statistics of numerical values of parameters and RMS error based on the horizontal force response for the best 20 models are listed in table 4.2. The lateral behavior is captured quite fairly, with RMS errors of 0.4-0.7 kN, calculated on the horizontal force history with a maximum of 250 to 270 kN. The difference between the isolators is minor than for vertical tests.

Optimal values for horizontal stiffness parameters can be detected from scatterplots (figure 6, right). Sensitivity analysis run with Simlab (Saltelli et al., 2004) confirmed the scatterplot analysis, highlighting the primary importance of p_4, immediately followed by p_5, and the minor but still noticeable contribute of p_6. Moreover, looking at first best models, it is possible to detect a certain degree of interaction between parameters, very strong between p_4 and p_5, weaker between p_4 and p_6, and between p_5 and p_6.

The model response does not seem to be influenced by the variation of tilting stiffness parameters p_7 and p_8, for which optimal values cannot be found. Sensitivity analyses based on the RMS error of the force prediction do not seem to localize any best value for the rotational stiffness parameters. Considering the free body diagram of the bearing is quite clear that in symmetric conditions, the moment at the top and bottom of the bearing is given by simple equilibrium considerations, i.e. independently from the value of the rotational stiffness: the only quantity useful in defining optimal values for tilting stiffness would be a direct measure of the layers rotation, which depends on rotational stiffness, but it is not available at the present time. In the next experimental campaigns a measure of the layers rotation is envisaged.

Table 4.2 Horizontal test results: statistics of best 20 models

		p_4	p_5	p_6	p_7	p_8	*RMS* error [kN]
RBA72-1	Mean	1.38	0.57	3.49	1.06	0.00	0.47
	Std	0.275	0.084	0.650	0.610	0.214	0.049
	cov	19.93%	14.70%	18.66%	57.47%	19170.26%	10.47%
RBA72-2	Mean	1.37	0.54	3.73	1.11	0.01	0.67
	Std	0.266	0.098	0.726	0.535	0.224	0.025
	cov	19.37%	18.24%	19.47%	48.09%	3727.83%	3.74%

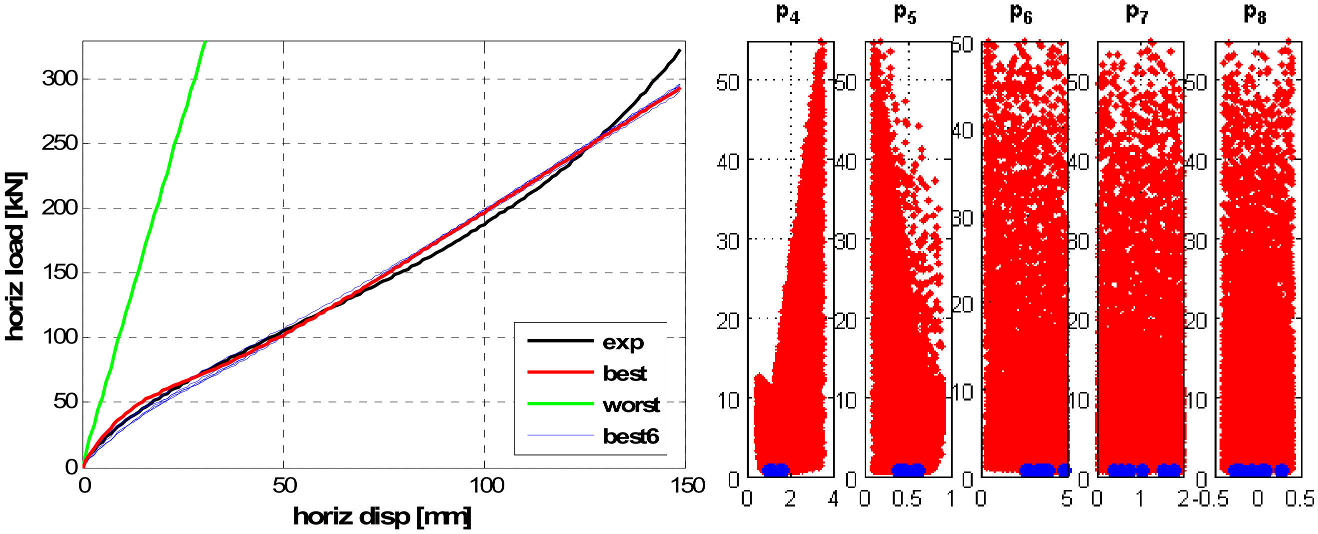

Figure 6 RBA72-2, test #2 (shear): best 8 models (left) and RMS scatterplots (right)

5. CONCLUDING REMARKS

After the first set of analyses, the model is found suitable to globally represent the overall isolator behavior. It is noted that some scatter is present in experimental data, i.e. statistically identical isolators present a certain degree of uncertainty in the mechanical response. The vertical and horizontal responses are fairly reproduced, even if at the present stage, a major lack of the model is the inability of simulating the horizontal stiffness hardening at large deformations, which is currently to be improved. A first screening of parameters by means of basic sensitivity analyses, allows withdrawing the followings:

1. The vertical stiffness model is found to be extremely dependent on the initial multiplier (p_1), whose optimal value is around the 20%.
2. concerning parameters p_2 and p_3, representing the nonlinear stiffness variation, a univocal localization could not be performed, even if a pattern has been detected in the RMS error which indicates that a more refined search of the model can likely given a more defined localization for the two parameters.
3. Optimal values for horizontal stiffness parameters can be reasonably detected. Looking at best models, it is possible to detect some interaction between parameters. No important dependence is found between vertical and horizontal response, at least in the ranges of isolator stability.
4. Optimal values of the initial horizontal stiffness multiplier (p_4) range around 135%.
5. The important reduction of the initial vertical stiffness and the increment of the initial shear stiffness with respect to the values obtained from relationships present in literature, can be explained considering that such relationships are representative not of the very beginning value of the stiffness, but of the average

stiffness in the medium deformation range, where the former has hardened and the latter has softened. For this reason, estimates found in literature for stiffness can be suitable for simplified linear models, but they have to be characterized differently for complex models including nonlinearity effects.
6. Rotational stiffness parameters p_7 and p_8 could not be calibrated, due to the lack of experimental rotation data along the bearing height. The calibration of rotational stiffness is envisaged in the next experimental campaign, since the rotational deformation state along the bearing height is strictly related to the rubber layers tear resistance and may be crucial in assessing the bearing failure modes.
8. Both vertical and horizontal calibrations revealed dominant parameters, at least at a first level sensitivity analysis. Higher level sensitivity analysis (variance based) is currently under study to assess the degree of influence of different parameters on the model and to detect interactions among parameters.

REFERENCES

Ali, H.M. and Abdel-Ghaffar, A.M. (1995). Modeling of rubber and lead passive-control bearings for seismic analysis. *Journal of Structural Engineering* , 1134-1144.
Benzoni, G., Casarotti, C. (2005). Effects of Vertical Load and Velocity on the Isolation Bearing Performance. Lead-rubber Bearings. paper #07-503, *Caltrans Bridge Research Conference 2005*, Sacramento CA.
Chang, C. (2002). Modeling of laminated rubber bearings using an analytical stiffness matrix. *International Journal of Solids and Structures* **39**, 6055–6078.
Doudoumis, I.N., Gravalas, F., Doudoumis, N.I. (2005). Analytical modeling of elastomeric lead-rubber bearings with the use of finite element micromodels. *5th GRACM Intnl Congr. Comp. Mechanics*, Limassol.
Hwang, J.S. and Hsu, T.Y. (2001). A fractional derivative model to include effect of ambient temperature on HDR bearings. *Engineering Structures* **23**, 484–490.
Hwang, J.S., Wu, J.D., Pan, T.-C., Yang, G. (2002).A mathematical hysteretic model for elastomeric isolation bearings. *Earthquake Engineering & Structural Dynamics* **31**,771–789.
Iizuka, M. (2000). A macroscopic model for predicting large-deformation behaviors of laminated rubber bearings. *Engineering Structures* **22**, 323-334.
Jaishi, B., Ren, W.X. (2007). Finite element model updating based on eigenvalue and strain energy residuals using multiobjective optimisation technique. *Mechanical Systems and Signal Processing* **21**, 2295–2317.
Kikuchi, M. and AIKEN, I. D. (1997). An analytical hysteresis model for elastomeric seismic isolation bearings. *Earthquake Engineering & Structural Dynamics* **26**, 215–231.
Koh, C.G., and Kelly, J.M. (1988). A simple mechanical model for elastomeric bearings used in base isolation. *International Journal of Mechanical Science*, **30:12**, 933-943.
Nagarajaiah, S., and Ferrell, K. (1999). Stability of elastomeric seismic isolation bearings. *ASCE Journal of Structural Engineering*, **125**, 946-954.
Ryan, K.L., Kelly, J.M., Chopra, A.K. (2005). Nonlinear Model for Lead–Rubber Bearings Including Axial-Load Effects. *Journal of Engineering Mechanics*, 1270-1278.
Takhirov, S.M. and Kelly, J.M. (2006). Numerical Study on Buckling of Elastomeric Seismic Isolation Bearings. *Proceedings of the 2006 Structures Congress*, St. Louis, Missouri
Yakut, A. and Yura, J.A. (2002). Parameters Influencing Performance of Elastomeric Bearings at Low Temperatures. *Journal of Structural Engineering*, 986-994.
Yoo, B., Lee, J.H., Koo, G.H., Lee, H.Y., Kim, J.B. (2000). Seismic base isolation technologies for Korea advanced liquid metal reactor. *Nuclear Engineering and Design* **199**, 125-142.
Saltelli, A., Tarantola, S., Campolongo, F., Ratto, M. (2004). Sensitivity analysis in practice: A guide to assessing scientific models, John Wiley & Sons.
Skinner, R.I, Robinson, W.H., McVerry, G.H, (1993). An introduction to seismic isolation, John Wiley & Sons.
Tarantola, A. (2004). Inverse Problem Theory and Methods for Model Parameter Estimation. SIAM.
The MathWorks, Inc. MATLAB (2007). The Math Works, Inc.: Natick, MA.
Zienkiewicz, O.C. and Taylor, R.L. (2000). The Finite Element Method, Fifth edition, Volume 1: The Basis. Butterworth-Heinemann